

MASTER

first line of text, except on page 1

SCIL-STRUCTURE INTERACTION EFFECTS ON THE RELIABILITY  
EVALUATION OF REACTOR CONTAINMENTS\*

BNL-NUREG--38048

J. Pires, H. Hwang and M. Reich\*\*

TI86 011198

### ABSTRACT

The probability-based method for the seismic reliability assessment of nuclear structures, which has been developed at Brookhaven National Laboratory (BNL)[1,2], is extended to include the effects of soil-structure interaction. A reinforced concrete containment building is analyzed in order to examine soil-structure interaction effects on: (1) structural fragilities; (2) floor response spectra statistics; and (3) correlation coefficients for total acceleration responses at specified structural locations.

### INTRODUCTION

To include the effect of soil flexibility on the reliability assessment of nuclear structures under earthquake loads, the following two-step approach is used. In the first step, the lumped parameter method for soil-structure interaction analysis is used together with a stick model representing the structure, in order to obtain the motions of the foundation plate. These motions, which include both translations and rotations of the foundation plate, are expressed in terms of the power-spectral density of the free-field ground excitation and the transfer function of the total acceleration response of the foundation. The second step involves a detailed finite element model of the structure subjected to the interaction motions computed from step one. Making use of this structural model and interaction motions the reliability analysis method yields the limit state probabilities and fragility data for the structure.

Text margin ►

### RELIABILITY ANALYSIS METHOD

An important ingredient for the reliability analysis is the identification of limit states. A limit state represents a state of undesirable structural behavior. In general, a limit state is defined from the actual structural behavior under loads. For a particular system, more than one limit state may be considered. For containment structures, the following limit states have been investigated: (1) flexure limit state[1,2], and (2) tangential shear limit state.[3,4]

\*This work was performed under the auspices of the U.S. Nuclear Regulatory Commission.

\*\*Brookhaven National Laboratory, Upton, NY 11973 USA

EPA/B

The flexure limit state is reached when the maximum compressive strain at the extreme fiber of the cross-section is equal to 0.003, while yielding of the extreme rebars in tension is permitted up to a strain of  $2f_y/E_s$ , where  $f_y$  and  $E_s$  are the yield strength and modulus of elasticity of the steel, respectively.

The ultimate tangential shear strength,  $V_u$ , is given by  $V_u = V_c + V_{so} + V_{si}$ , where  $V_c$  is the tangential shear strength provided by concrete,  $V_{so}$  is the tangential shear strength provided by the orthogonal reinforcement and  $V_{si}$  is the tangential shear strength provided by diagonal reinforcement. Usually the shear strength  $V_u$  is expressed in units of stress, which is achieved dividing  $V_u$ ,  $V_c$ ,  $V_{so}$  and  $V_{si}$  by  $(bt)$  to obtain  $v_u$ ,  $v_c$ ,  $v_{so}$  and  $v_{si}$ , respectively, where  $b$  is the unit length and  $t$  the thickness of the cross section. Under normal tensile membrane stress it is

$$v_c = 0$$

$$v_{so} = \rho_0 f_y (1 - f_s/f_y) \quad (1)$$

$$v_{si} = \rho_1 f_y$$

where  $\rho_0$  is the orthogonal reinforcement ratio and  $\rho_1$  is the diagonal reinforcement ratio. Equation 1 assumes that the diagonal reinforcement resists shear exclusively. Under normal compressive membrane stress

$$v_c = 0$$

$$v_u = (\rho_0 + \rho_1) f_y \quad (2)$$

In addition, the maximum shear stress can not exceed  $0.25 f'_c$ .

On the basis of the limit states defined above, a limit state surface can be constructed for a cross-section with a specific geometry and reinforcement arrangement.

Text margin

In the reliability analysis, the limit state probabilities are evaluated considering the randomness and uncertainties in the loads, structural resistance and soil properties. The dead load is considered deterministic and constant during the life of the structures. The earthquake loads are random and modeled as a Gaussian process with an appropriate spectrum. Uncertainties in the strength of concrete and reinforcement, and in the shear modulus and material damping of the soil are included in the reliability assessment using the Latin hypercube sampling technique.<sup>[5]</sup>

For the dead load, the finite element technique is used to evaluate the element stress resultants. For the earthquake load, characterized by its cross-spectral density matrix and duration of the strong motion phase, the finite element analysis is used to evaluate the dynamic characteristics of the structure, i.e., the mode shapes and frequencies of free vibration. Using these characteristics and the random vibration theory, the structural response

is obtained in the form of a cross-spectral density matrix, which upon integration produces a response second moment cross-correlation matrix.

Under the assumption that the earthquake load and structural response to earthquakes are Gaussian, techniques for estimating the rate at which a response vector outcrosses the limit state surfaces have been established.[1] This outcrossing rate can, in turn, be used to evaluate the conditional limit state probabilities of the structure subjected to the given combination of earthquake and dead load.

#### SOIL-STRUCTURE INTERACTION ANALYSIS

The equations of motion for the lumped parameter model of the soil-structure system are formulated following the procedure outlined in Ref. 6. With this procedure, a coordinate system that dynamically couples and statically uncouples the soil-structure system is chosen. This is desirable, since different variabilities are usually associated with the structure stiffness and foundation-soil interaction parameters. Furthermore, it also allows for the use of the fixed-base modes of vibration in the analysis, thus reducing the number of unknowns in the equation of motion.

A frequency domain solution for the equations of motion is used. The solution obtained is the transfer function vector which relates the translational and rotational responses of the foundation plate to the free-field ground motion. Once the transfer function of the foundation motions is obtained, the cross-spectral density matrix of the foundation acceleration response can be obtained in terms of the power spectrum of the free-field ground acceleration. This cross-spectral density matrix is then used as input for a detailed finite element model of the fixed-base structure for the calculation of the structural fragilities. For the computation of the floor response spectra statistics the simplified stick model can be used. In this manner, the two step approach required for the structural fragility evaluation is not required for floor response spectra calculations.

Text margin

In the derivation of the equations of motion for the entire soil-structure system no assumptions are made as to the type of halfspace to be used. The halfspace could homogeneous or nonhomogeneous, horizontally layered or uniform. In general, a three-dimensional representation of the halfspace is necessary. In the frequency domain, the interface forces  $P$  and  $Q$  are related to the magnitude of the base sliding  $u_b$  and  $\psi$  through the impedance functions. For the case of a circular rigid disc on a halfspace several solutions have been reported.[7,8] Following the working Ref. [7] the force amplitudes  $P$  and  $Q$  corresponding to the displacements  $u_b$  and  $\psi$  are expressed as follows:

$$\begin{Bmatrix} P \\ Q \end{Bmatrix} = \begin{bmatrix} K_{xx}^0 (K_{11} + ia_0 C_{11}) & K_{x\psi}^0 (K_{12} + ia_0 C_{12}) \\ K_{x\psi}^0 (K_{12} + ia_0 C_{12}) & K_{\psi\psi}^0 (K_{22} + ia_0 C_{22}) \end{bmatrix} (1+2i\beta) \begin{Bmatrix} u_b \\ \psi \end{Bmatrix} \quad (3)$$

where  $K_{xx}^0$ ,  $K_{x\psi}^0$ ,  $K_{\psi\psi}^0$  have dimensions of stiffness and depend on the foundation radius,  $R$ , S-wave velocity in the halfspace,  $V_s$ , and Poisson's ratio  $\nu$ . The expressions used for those stiffness were those given in Ref. [7]. The  $K$ 's and  $C$ 's are dimensionless quantities that depend on the Poisson's ratio  $\nu$ , the foundation radius and the frequency parameter  $a_0 = \omega R/V_s$ , where  $\omega$  is the frequency in radians per second. Expressions for the calculation of the dimensionless coefficients  $K$  and  $C$  are also given in Ref. [7]. The quantity  $\beta$  in Eq. 3 is the hysteretic damping in the soil expressed as a percent of the initial viscous damping ratio. Finally,  $i$  denotes the complex number  $\sqrt{-1}$ . In addition to the sliding and rocking springs, a vertical and a torsional spring are also necessary. Vertical and torsional modes of vibration, however, were not included in the example described in this paper.

#### CONTAINMENT BUILDING AND SOIL DEPOSIT

The reinforced concrete containment structure consists of a circular cylindrical wall, a hemispherical dome and a circular foundation plate as shown in Fig. 1. The containment wall is reinforced with hoop and meridional rebars in two layers, one in the vicinity of the internal surface and the other near the external containment surface. Details of the containment reinforcement can be found in Ref. [9]. The concrete uniaxial compressive strength is considered to follow a Gaussian distribution with a mean of 6,085.6 psi and a standard deviation of 650.5 psi. The Young's modulus and Poisson's ratio for the concrete are taken as  $3.6 \times 10^6$  and 0.20, respectively. For the reinforcing steel a lognormal distribution with a mean of 71,100 psi and a standard deviation of 2,570 psi is considered appropriate. The Young's modulus and Poisson's ratio for the steel are  $29 \times 10^6$  psi and 0.3, respectively.

A three-dimensional finite element model of the containment was constructed using thin shell finite elements. Under the dead load the stresses in the containment were calculated using this model. With that same model the first twenty natural frequencies and mode shapes were determined. The frequencies of the first two pairs of bending modes, the significant modes for the containment response to earthquakes are 2.97 cps and 8.82 cps, respectively. To account for cracking of the concrete the stiffnesses of the elements in the containment model are taken to be one half of those of the uncracked sections.

For the soil-structure interaction analysis, a simplified model of the containment and internal structures is used in Fig. 2. The internal structures are: the drywell, the reactor pedestal and the reactor shield wall. The simplified structural model is the so-called stick model which consists of beam elements. Included in the stick model are the masses and, rotational inertias of the reactor and sump floor. For the internal structures the uncracked stiffnesses were used.

The soil deposit beneath the structural foundation has been idealized as an homogeneous soil deposit. The mean S and P-waves velocities in the soil are 1,100 ft/sec and 5,700 ft/sec, respectively. A lognormal distribution with a mean of  $1.0 \times 10^7$  ksf and a CoV of 0.7 is used for the

shear modulus.[9,10] For the hysteretic damping ratio a lognormal distribution with a mean of 0.075 and a CoV 1.0 is considered appropriate. [9,10] The Poisson's ratio for the soil is 0.45, and the dry-and-wet unit weight are 138pcf and 150pcf, respectively. It is well known that the dynamic stress-strain behavior of soils is highly nonlinear. Instead of performing nonlinear dynamic analysis for the soil-structure interaction, it has been customary to use one-dimensional wave propagation analysis and an equivalent linearization technique (SHAKE analysis[11]), in order to obtain the soil properties to be used in the soil-structure interaction analysis. For the reliability analysis this would have to be done for several levels of earthquake intensity since all ground shaking intensities that are likely to occur at the site must be included in the reliability evaluation. Since consideration of nonlinear effects is beyond the scope of this study, only one set of soil properties are used in the analysis. A mean value of the soil stiffness that corresponds to one half of the initial tangent stiffness is chosen, as well as the corresponding mean damping ratio.

#### EARTHQUAKE LOAD

The ground acceleration at the free-field, on the condition that an earthquake occurs, is idealized as a segment of a stationary filtered white noise random process with zero-mean, described in the frequency domain by its power spectral density  $S_g(\omega)$ . The power spectral density,  $S_g(\omega)$ , of an earthquake is site-specific. In this study, the power spectrum of the earthquake ground acceleration is obtained from the site-specific response spectrum using the method described in Appendix B of Ref. 9. An analytical form for the power spectrum is chosen, and the random vibration theory is used to calculate the response spectrum, consistent with the chosen power spectrum. An optimization technique is used to determine the parameters of the analytical form for the power spectrum, that minimize the difference between the site-specific response spectrum and the response spectrum consistent with the proposed power spectrum. It should be emphasized that only the shape of the power spectrum is obtained with this technique, and that the frequency content of the ground acceleration remains unchanged for the peak ground acceleration range defined by the seismic hazard.

In this study, it has been observed that the following form for the power spectrum

$$S_g(\omega) = S_0 \sum_{i=1}^2 p_j \frac{(1+4\zeta_j^2)[1-\exp(-\omega^4/\omega_j^4)]}{[1-(\omega/\omega_j)^2]^2 + 4\zeta_j^2(\omega/\omega_j)^2} \quad (4)$$

may be a better representation of the ground motions at a site than the so-called Kanai-Tajimi spectrum. The spectrum of Eq. 4 has a lower high frequency content than the Kanai-Tajimi spectrum, and the ratio  $S_g(\omega)/\omega^4$  tends to a finite value as  $\omega$  approaches zero. The site-specific response spectrum at the site is shown in Fig. 3, and the proposed

power spectrum is shown in Fig. 4. The response spectrum consistent with the proposed power spectrum is compared in Fig. 3 with the specified site-specific response spectrum.

LAST LINE OF PAPER TITLE

## STRUCTURAL FRAGILITIES

Fragility curves are defined as a plot of the conditional limit state probability for a peak ground acceleration  $A_1=a$ . Fragility curves for both the tangential shear and bending limit states were computed with and without consideration of soil-structure interaction effects.<sup>[9]</sup> As an example, the fragility curves for the tangential shear limit state with and without soil-structure interaction effects are shown in Fig. 5. The median and range of the fragility curves shown in Fig. 5 are given in Table 1 below. In Table 1 the upper bound corresponds to a probability of failure of 0.937, the lower bound to a probability of failure 10<sup>-11</sup>.

TABLE 1  
Median and Range of Tangential Shear Fragility (in g's)

Condition	Median	Lower Bound	Upper Bound
Fixed-base	1.60	0.57	2.29
Interaction	1.87	0.56	Abstract margin 2.75

As can be seen from Fig. 5 and Table 1, the soil-structure interaction increases the median of the fragility, and its dispersion as measured by the fragility range. For the bending limit state the effects of soil-structure interaction were similar to those for the tangential shear limit state.

## FLOOR RESPONSE SPECTRA

Floor response spectra statistics were computed for the fixed-base and interaction conditions. In particular, the mean floor response spectra and the coefficients of variation of (CoV) of the floor response spectra ordinates have been computed. The mean and CoV floor response spectra at the top of the containment building are shown in Figs. 6 and 7 respectively. The floor response spectra for the interaction and fixed-base condition are markedly different. For the interaction condition the spectral ordinates are always smaller than those for the fixed-base condition for frequencies above 1.5 cps, and the predominant spectral frequency for the interaction condition is lower than that for the fixed-base. The CoV's of the floor response spectra ordinates for the interaction condition are much larger than those for the fixed-base, especially for frequencies between 1.5 and 3.0 cps which is the range of interaction frequencies for the various Latin hypercube samples.

The correlation matrices for the total acceleration response at four locations, namely nodes 1,2, 6 and 14 (see Fig. 2) are shown in Table 2, below.

TABLE 2  
Acceleration Responses Correlations

(a) Fixed-base

Node	1	2	6	14
1	1.0	.9921	.3855	-0.09524
2	.9921	1.0	.4779	-0.07749
6	.3855	.4779	1.0	.3651
14	-0.09524	-0.07749	.3651	1.0

(b) Interaction

Node	1	2	6	14
1	1.0	.8980	.2468	-.2349
2	.8980	1.0	.5369	-.1583
6	.2468	.5369	1.0	.4753
14	-.2349	-.1583	.4753	1.0

Correlation coefficients between the floor response spectra ordinates can also be easily computed with the proposed approach.

#### CONCLUDING REMARKS

This paper presents a reliability analysis method in which soil structure interaction effects have been included. Structural fragilities for a reinforced concrete containment obtained with the method show that the soil-structure interaction increases the median and range of the structural fragility. Computation of floor response spectra statistics for the example structure have shown that the mean and coefficient of variation of the floor response spectra ordinates are markedly affected by the interaction effect.

#### REFERENCES

- [1] Shinozuka, M., Hwang, H., and Reich, M., "Reliability Assessment of Reinforced Concrete Containment Structures", Nuclear Engineering and Design, 80 (1984) 247-267.
- [2] Kawakami, J., et al., "Reliability Assessment of Indian Point Unit 3 Containment Structure", NUREG/CR-3641, January 1974.
- [3] Oesterle, R.G., "Tangential Shear Design in Reinforced Concrete Containments - Research Results and Applications", Nuclear Engineering and Design, 79 (1984) 161-168.

[4] Pepper, S., et al, "Reliability Assessment of Containment Tangential Shear Failures", BNL/NUREG-51913.

[5] Iman, R.L., and Conover, W.J., "Small Samples Sensitivity Analysis Techniques for Computer Models, With an Application to Risk Assessment", Communications in Statics: Theory and Methods, Vol. A9, No. 17, pp. 1749-1842, 1980.

[6] Hamilton, C.W., and Hadjian, A.H., "Probabilistic Frequency Variations of Structure-Soil Systems", Nuclear Engineering and Design, 38 (1976), 303-322.

[7] Kausel, E., et al., "The Spring Method for Embedded Foundations", Nuclear Engineering and Design, 48 (1978), pp. 377-392.

[8] Hall, J.R. and Kisselkennig, J.E., "Special Topics in Soil Structure Interaction", Nuclear Engineering and Design, 38 (1976) 273-287.

[9] Pires, J., Hwang, H., and Reich, M., "Reliability Evaluation of Containments Including Soil-Structure Interaction", NUREG/CR-4329 (in preparation).

[10] Bohn, M.P., et al., "Application of the SSMRP Methodology to the Seismic Risk at the Zion Nuclear Power Plant", NUREG/CR-3428, January 1984.

[11] Schnabel, P.B., and Lysmer, J., "SHAKE: A Computer Program for Earthquake Response Analysis of Horizontally Layered Soil Sites", Earthquake Engineering Research Center, EERC/72-12, U.C., Berkeley, California, 1972.

#### NOTICE

This work was performed under the auspices of the U.S. Nuclear Regulatory Commission, Washington, D.C. The findings and opinions expressed in this paper are those of the authors, and do not necessarily reflect the views of the U.S. Nuclear Regulatory Commission or Brookhaven National Laboratory.

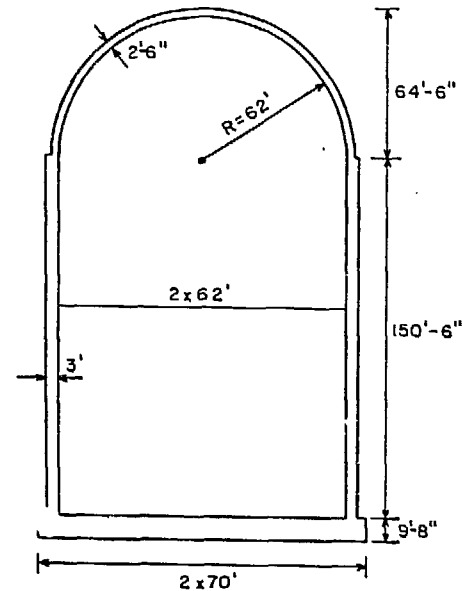


Fig. 1 Containment

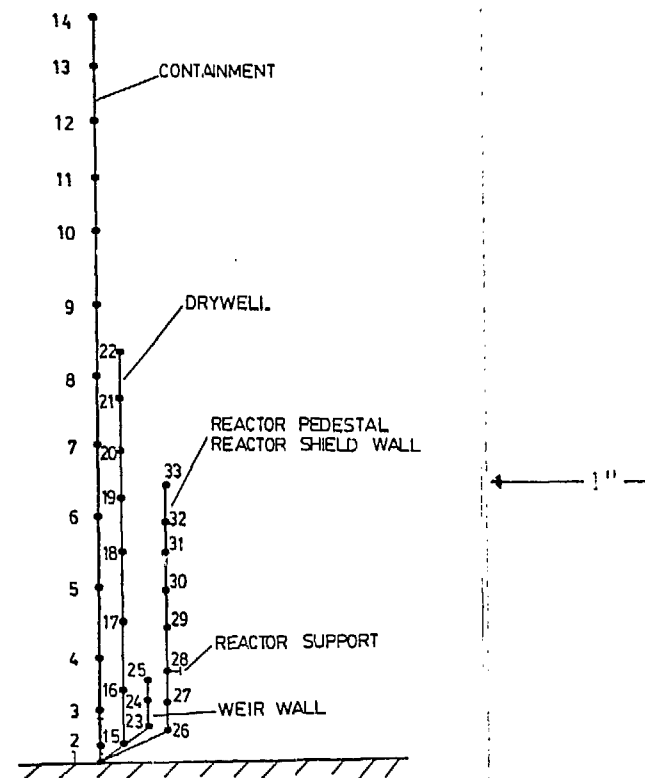


Fig. 2 Stick Model

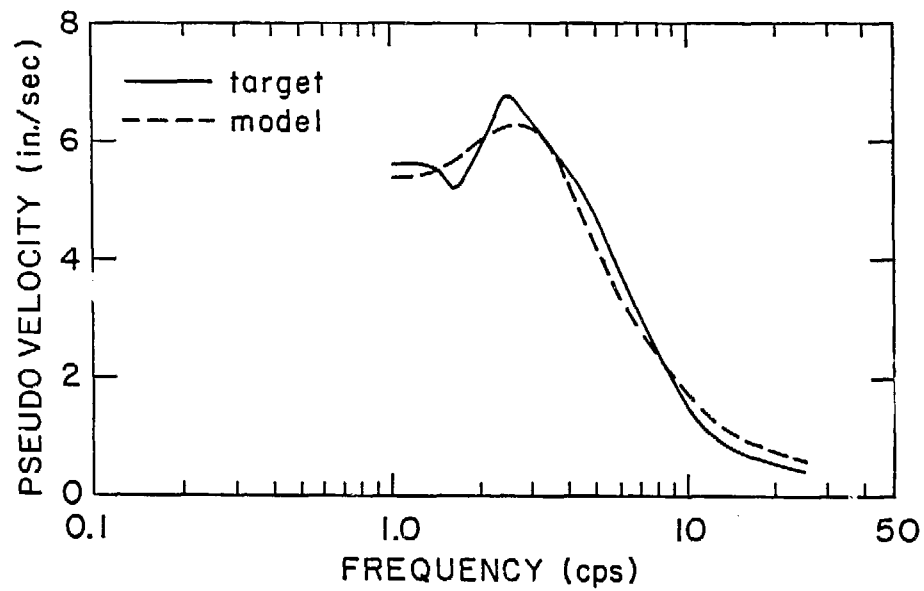


Fig. 3 Site-Specific Response Spectrum

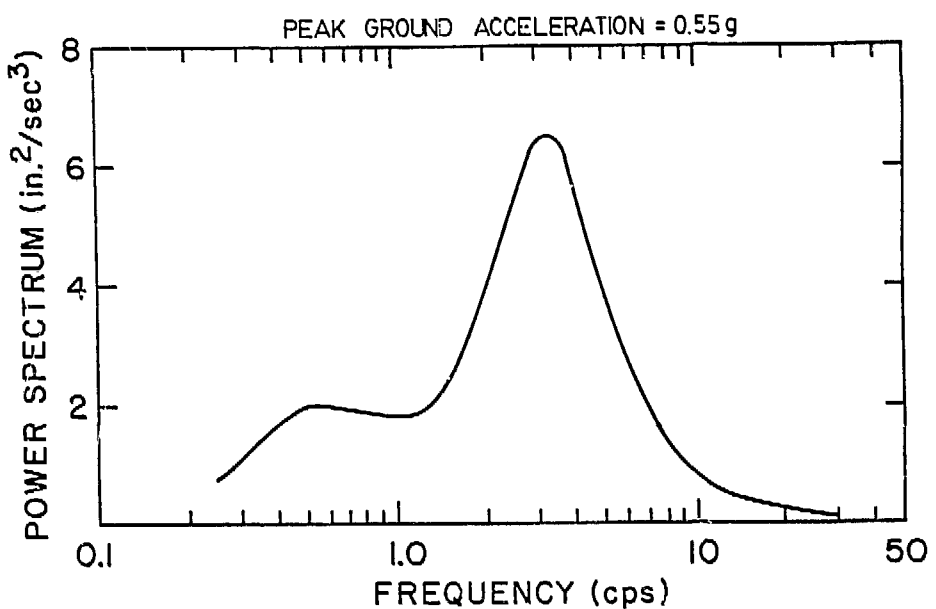


Fig. 4 Power Spectrum

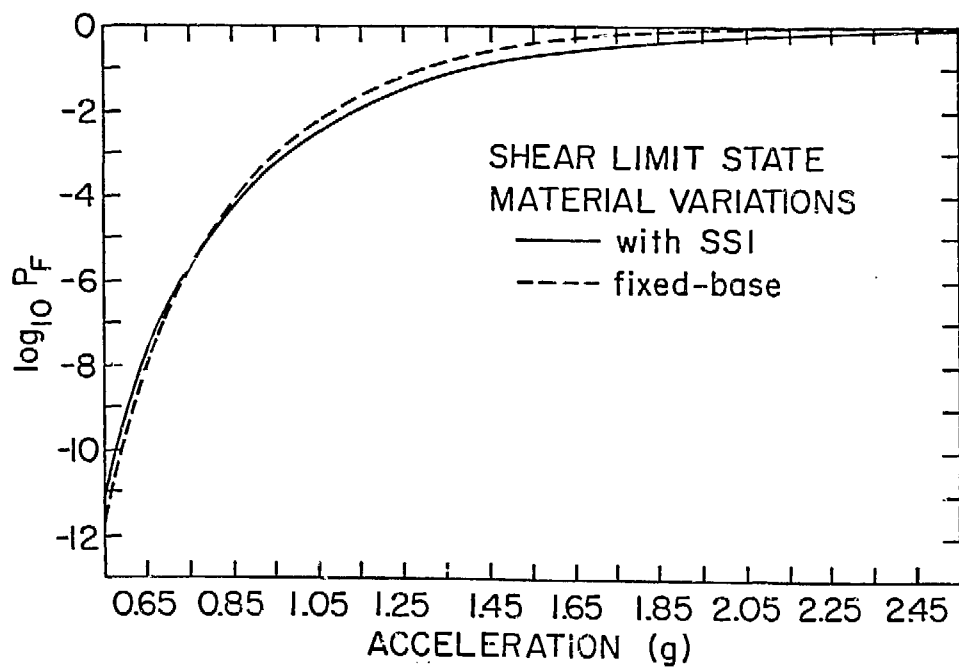


Fig. 5 Fragility Curves

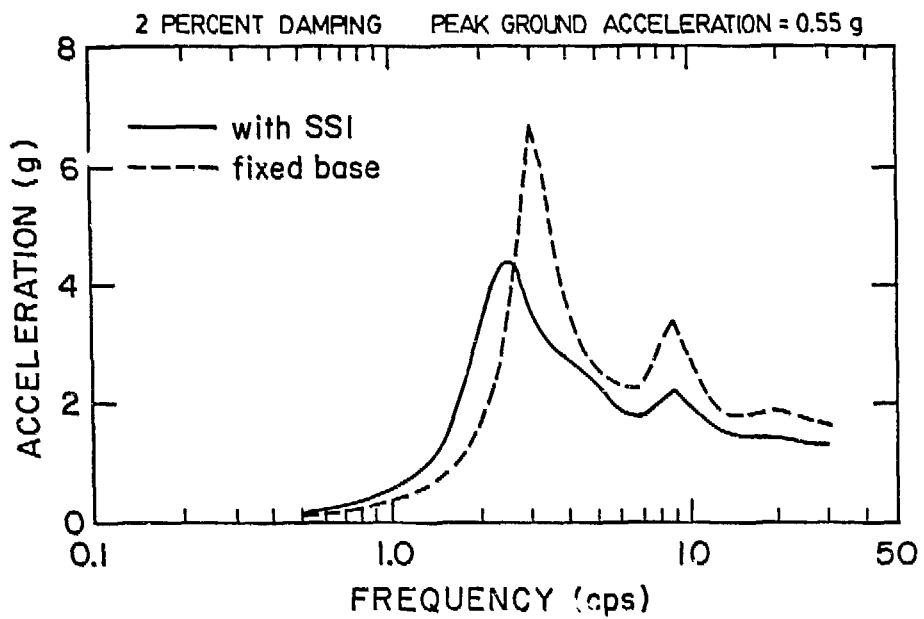


Fig. 6 Mean Floor Response Spectra

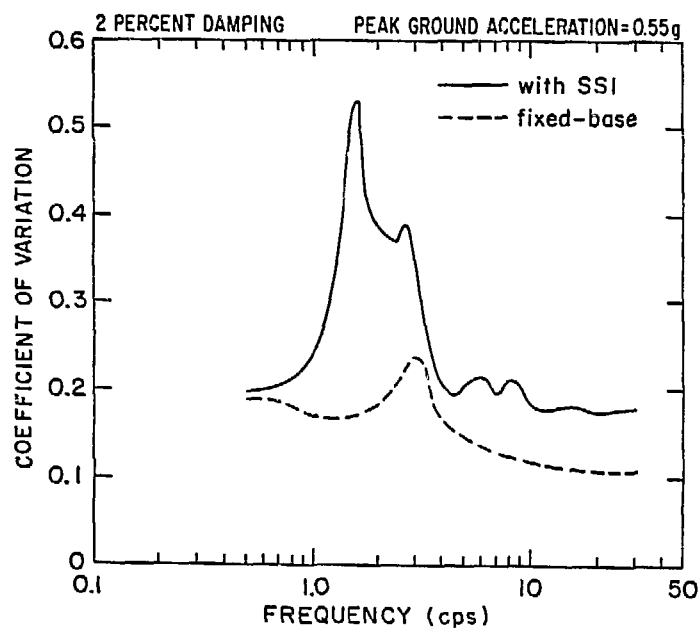


Fig. 7 CoV of Floor Response Spectra